Short Article

Developmental Cell

# Localized Smooth Muscle Differentiation Is Essential for Epithelial Bifurcation during Branching Morphogenesis of the Mammalian Lung

## Graphical Abstract

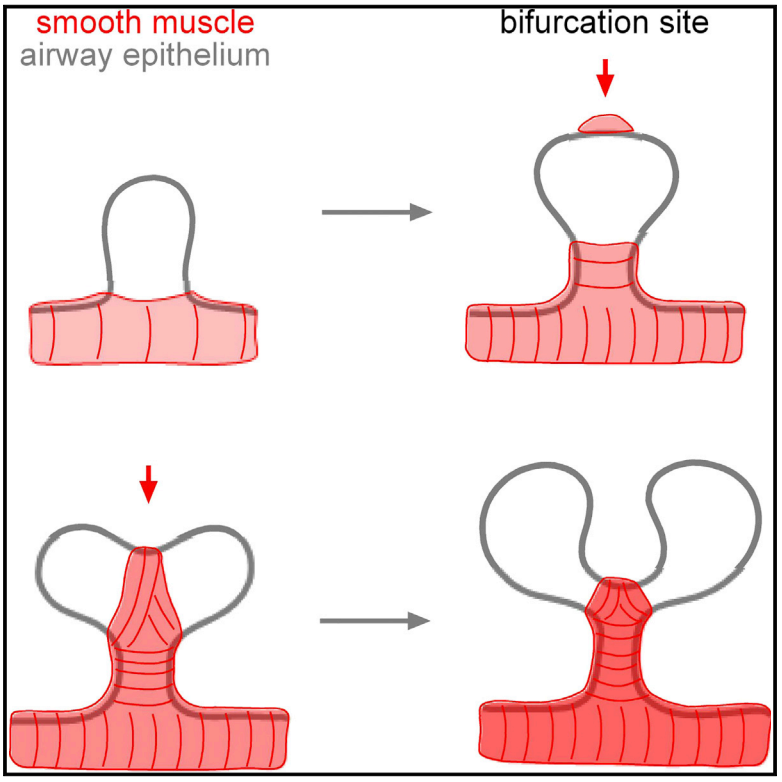


## Authors

Hye Young Kim, Mei-Fong Pang, Victor D. Varner, ..., Erin Miller, Derek C. Radisky, Celeste M. Nelson

## Correspondence

celesten@princeton.edu

## In Brief

Epithelial morphogenesis is influenced by soluble signals from the surrounding mesenchyme, but the physical role of this tissue is unknown. Here, Kim, Pang et al. show that stereotyped differentiation of smooth muscle is required for branching morphogenesis of the airway epithelium in the mammalian lung.

## Highlights

- Regions of epithelial shape change coincide with differentiating smooth muscle
- Differentiating smooth muscle cells appear at lung bud bifurcation sites
- Blocking differentiation or surgically removing smooth muscle disrupts bifurcation

Kim et al., 2015, Developmental Cell *34*, 719–726
September 28, 2015 
http://dx.doi.org/10.1016/j.devcel.2015.08.012

CellPress

Developmental Cell
Short Article

# Localized Smooth Muscle Differentiation Is Essential for Epithelial Bifurcation during Branching Morphogenesis of the Mammalian Lung

Hye Young Kim,[1,4] Mei-Fong Pang,[1,4] Victor D. Varner,[1] Lisa Kojima,[1] Erin Miller,[3] Derek C. Radisky,[3] and Celeste M. Nelson[1,2,*]
[1]Department of Chemical and Biological Engineering, Princeton University, Princeton, NJ 08544, USA
[2]Department of Molecular Biology, Princeton University, Princeton, NJ 08544, USA
[3]Department of Cancer Biology, Mayo Clinic Cancer Center, Jacksonville, FL 32224, USA
[4]Co-first author
*Correspondence: celesten@princeton.edu
http://dx.doi.org/10.1016/j.devcel.2015.08.012

## SUMMARY

**The airway epithelium develops into a tree-like structure via branching morphogenesis. Here, we show a critical role for localized differentiation of airway smooth muscle during epithelial bifurcation in the embryonic mouse lung. We found that during terminal bifurcation, changes in the geometry of nascent buds coincided with patterned smooth muscle differentiation. Evaluating spatiotemporal dynamics of α-smooth muscle actin (αSMA) in reporter mice revealed that αSMA-expressing cells appear at the basal surface of the future epithelial cleft prior to bifurcation and then increase in density as they wrap around the bifurcating bud. Disrupting this stereotyped pattern of smooth muscle differentiation prevents terminal bifurcation. Our results reveal stereotyped differentiation of airway smooth muscle adjacent to nascent epithelial buds and suggest that localized smooth muscle wrapping at the cleft site is required for terminal bifurcation during airway branching morphogenesis.**

## INTRODUCTION

The developing lung begins as a simple epithelial tube surrounded by thick mesenchyme. New buds emerge sequentially along the length of the epithelial tube via domain branching, while the tip of the elongated tube bifurcates to form two daughter buds (Metzger et al., 2008). Repetition of these bifurcations at defined angles (planar or orthogonal to the long axis of the parent tube) generates the stereotyped, hierarchically organized three-dimensional (3D) branched architecture of the lung (Metzger et al., 2008). Pioneering tissue grafting studies revealed that the mesenchyme provides inductive cues for the branching epithelium (Alescio and Cassini, 1962; Grobstein, 1953), and several signaling molecules have since been identified including fibroblast growth factor (FGF)-9, FGF10, bone morphogenetic protein (BMP)-4, and sonic hedgehog (SHH) (reviewed in Metzger and Krasnow, 1999 and Morrisey and Hogan, 2010). However, a possible connection between patterns of mesenchymal differentiation and airway epithelial branching has remained largely unexplored.

During morphogenesis of the lung, the mesenchyme differentiates into several cell types, including smooth muscle, vasculature, and nerves that envelop the entire airway epithelium as it branches (McCulley et al., 2015; Schachtner et al., 2000; Sparrow and Lamb, 2003; Tollet et al., 2001). Among these, the airway smooth muscle forms tightly packed bundles around the circumference of the epithelium in a cranial to caudal direction along the primary bronchus (Sparrow and Lamb, 2003). After the smooth muscle forms, it contracts spontaneously in a peristaltic wave, narrowing the airways and pushing luminal fluid toward the terminal ends (Featherstone et al., 2005; Jesudason et al., 2005; Schittny et al., 2000). Although the presence of airway smooth muscle and its contractile behaviors have been observed in several species (Featherstone et al., 2005; Lewis, 1924; McCray, 1993; Schittny et al., 2000), its role in patterning airway branching has not been defined (Jesudason et al., 2005; Unbekandt et al., 2008).

Here, we identified a role for stereotyped differentiation of airway smooth muscle in branching morphogenesis of the embryonic mouse lung and found that terminal bifurcations of the epithelium require the localized presence of smooth muscle at the cleft site. Time-lapse imaging of embryonic mouse lung explants revealed that changes in the shape of the epithelial bud coincide with patterned differentiation of smooth muscle. Remarkably, we found, using a transgenic reporter mouse, that α-smooth muscle actin (αSMA)-expressing cells appear adjacent to the airway epithelium prior to its bifurcation and then increase in density as they wrap around the bifurcating cleft and neck of the bud. Disrupting patterns of smooth muscle differentiation abolishes terminal bifurcation of the epithelium. Furthermore, surgically removing the smooth muscle from the cleft causes the epithelium to pop back into an un-bifurcated geometry. These results reveal a major role for the spatial pattern of smooth muscle differentiation during terminal bifurcation of the airway epithelium.

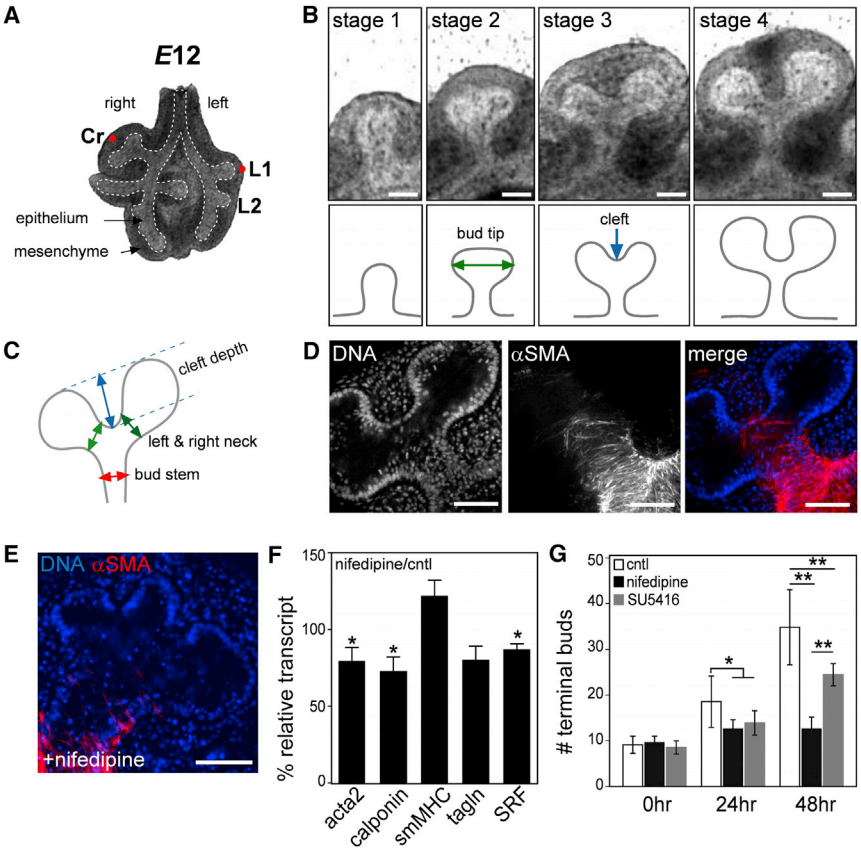


**Figure 1. Smooth Muscle Differentiation Is Required for Airway Epithelial Bifurcation**

(A) At *E*12, the embryonic mouse lung has two left (L1 and L2) buds, and the right cranial (Cr) lobe has started to bifurcate. The dotted line indicates the airway epithelium, which is surrounded by mesenchyme.

(B) Snapshots were taken from time-lapse movies. Scale bars, 100 μm.

(C) Morphometric parameters were used to quantify the kinematics of terminal bifurcation.

(D) Airway smooth muscle wraps around the bifurcating neck. Scale bars, 50 μm.

(E and F) Smooth muscle differentiation is inhibited using nifedipine (10 μM). Shown are staining and qRT-PCR analysis of the smooth muscle markers αSMA (acta2), calponin-1, smooth muscle myosin heavy chain (smMHC), transgelin (tagln; SM22α), and the transcription factor SRF. Shown are mean ± SD for three independent experiments. Scale bar, 50 μm.

(G) Branching morphogenesis was quantified as the number of terminal buds after drug treatment. Shown are mean ± SD for $n \geq 9$ for each condition; $^{*}p < 0.05$; $^{**}p < 0.01$.

See also Figure S1 and Movies S1 and S2.

## RESULTS

### Terminal Bifurcation of the Airway Epithelium Is Accompanied by Smooth Muscle Differentiation

The branched architecture of the mammalian lung is sculpted in part by repeated bifurcations of the terminal ends of the growing airways (Metzger et al., 2008). To follow the dynamics of tissue morphogenesis during terminal bifurcation, we imaged the branching of lungs explanted from *E*12 mouse embryos in real time (Figure 1A; Movie S1). At this stage of development, terminal bifurcations proceeded through a stereotyped sequence of events: the nascent epithelial bud first swelled at its tip (stage 1), it flattened (stage 2), and then a cleft appeared at the midline (stage 3; Figure 1B). The cleft then deepened as each side of the bifurcation elongated (stage 4). Quantitative morphometric analysis (Figure 1C) revealed that the stem of the bud narrowed as the tip swelled (Figure S1A), and the neck of each side of the bifurcating bud narrowed as the cleft deepened (Figure S1B), consistent with qualitative descriptions of bifurcation reported by others (Schnatwinkel and Niswander, 2013).

The narrowing of the stem and neck regions of the bud during terminal bifurcation suggested that these changes in epithelial shape might be influenced by the surrounding mesenchyme. Both the airway smooth muscle and the vascular endothelium actively differentiate from mesenchymal progenitors during lung development (Kumar et al., 2014; Schachtner et al., 2000; Tollet et al., 2001). Immunostaining for αSMA or platelet endothelial cell adhesion molecule (PECAM) revealed that both cell types were localized around the branching epithelium at *E*12.5 (Figure S1C). At areas actively undergoing bifurcation, the airway smooth muscle (Figure 1D; Movie S2) and the vascular endothelium (Figure S1D) appeared to wrap from the primary bronchus and up around the stem of the bud. To determine whether these mesenchymal cell populations are required for terminal bifurcation of the epithelium, we inhibited airway smooth muscle contraction using the L-type calcium channel blocker nifedipine (McCray, 1993; Roman, 1995) and blood vessel formation using the vascular endothelial growth factor receptor antagonist SU5416 (Fong et al., 1999). Inhibiting smooth muscle contraction both reduced the extent of smooth muscle differentiation (Figures 1E and 1F) and blocked terminal bifurcation of the epithelium (Figure 1G; Figure S1F). In contrast, although inhibiting vascular development significantly decreased the number of epithelial branches (Figures S1E and S1G), consistent with previously published work (Havrilak and Shannon, 2015; Lazarus et al., 2011), the absence of vasculature did not completely prevent terminal bifurcation of the epithelium (Figure 1G).

### Airway Smooth Muscle Localizes to the Cleft prior to Terminal Bifurcation

To investigate whether the pattern of airway smooth muscle plays an active role in epithelial bifurcation, we followed the dynamics of smooth muscle development using time-lapse imaging of embryonic lungs explanted from transgenic reporter mice that express red fluorescent protein (RFP) downstream of the αSMA promoter (αSMA-RFP) (Figure S2A) (Magness et al., 2004). Analysis of the spatiotemporal dynamics of the epithelium and smooth muscle revealed that the localized RFP signal first appears at the midline of the basal surface of the swollen bud

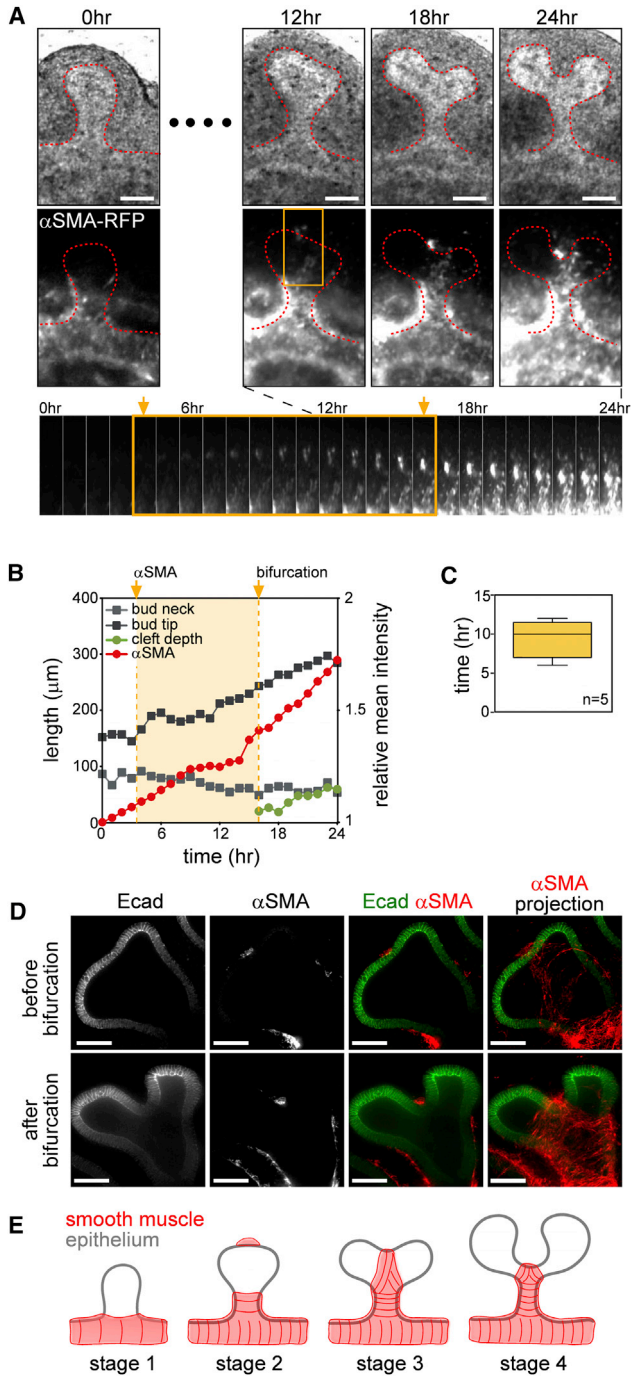


**Figure 2. Smooth Muscle Appears at Cleft Sites prior to Terminal Bifurcation**

(A) Snapshots from time-lapse movie of the αSMA-RFP lung explant. The kymograph shows the temporal sequence of αSMA expression from regions indicated in the yellow inset (12 hr). The airway epithelium is outlined by a dotted red line. Scale bars, 100 μm.

(B) Quantification of morphometric parameters and αSMA intensity as a function of time. The yellow shaded region indicates the duration of αSMA appearance at the bud tip prior to bifurcation. Arrows on top indicate the timing of the first appearance of αSMA (left yellow arrow) and terminal bifurcation (right yellow arrow). αSMA-RFP intensity was measured along the perimeter of the bud tip.

(C) Quantification of time-lapse movies showing average duration of appearance of αSMA-positive cells prior to the bifurcation (mean ± SD for five independent experiments).

(D) Immunostained buds before and after the terminal bifurcation. Scale bars, 50 μm.

(E) Schematic representation of smooth muscle localization during terminal bifurcation of the airway epithelium.

See also Figure S2 and Movie S3.

and then expands and increases in intensity at the bifurcating cleft and neck of the buds (Figure 2A; Movie S3). Thereafter, the intensity of the RFP signal continues to increase as the smooth muscle wraps around the entire neck of the bifurcating bud (Figure 2B). Strikingly, kymograph analysis of the area of the future cleft revealed that smooth muscle cells appear at the cleft site before the epithelial bifurcation begins (Figure 2A). This appearance of the αSMA-RFP signal at the future cleft site was observed consistently in multiple explants 8.6 ± 1.9 hr prior to bifurcation of the epithelium (Figure 2C). Immunofluorescence analysis of fixed specimens confirmed the presence of a small population of αSMA-positive mesenchymal cells that appear at the midline of the basal surface of the epithelial bud prior to the formation of the cleft (Figure 2D; Figures S2B–S2D). Based on these observations, we hypothesized that terminal bifurcation of the airway epithelium is directed by localized differentiation of smooth muscle cells (Figure 2E).

## Stereotyped Smooth Muscle Differentiation Is Required for Terminal Bifurcation

To determine whether localized differentiation of smooth muscle at the future cleft site is required for terminal bifurcation of the airway epithelium, we pharmacologically perturbed the pattern of smooth muscle differentiation around the nascent buds. Disrupting FGF signaling using a fibroblast growth factor receptor (FGFR) tyrosine kinase inhibitor (SU5402) (Mohammadi et al., 1997) or activating SHH signaling using smoothened agonist (SAG) (Chen et al., 2002b; Radzikinas et al., 2011) induced the formation of ectopic smooth muscle around the entire airway epithelium but with different spatial patterns. Treatment with SU5402 caused smooth muscle to wrap completely around the airway epithelium, with smooth muscle cells aligning in a direction perpendicular to that of bud extension (Figure 3A; Figures S3A and S3B) but without increasing the overall expression of markers of smooth muscle differentiation (Figure S3C). Development of this tightly wrapped smooth muscle appeared to block further epithelial branching, even after initial formation of the cleft (Figures 3A–3C; arrows in SU5402). In contrast, treatment with SAG led to randomly oriented ectopic smooth muscle throughout large regions of the mesenchyme, including the areas in between buds (Figure 3A; Figures S3A and S3B). The epithelium failed to bifurcate and instead formed several shallow buckles along its surface (Figure 3C). Ectopic smooth muscle thus prevented terminal bifurcation and inhibited normal branching morphogenesis.

Conversely, treatment with either nifedipine or SHH antagonist cyclopamine (Chen et al., 2002a) decreased smooth muscle differentiation (Figure S3C), which was limited to regions around the primary bronchus and absent from regions surrounding the bud (Figure 3A; Figure S3A). These treatments prevented

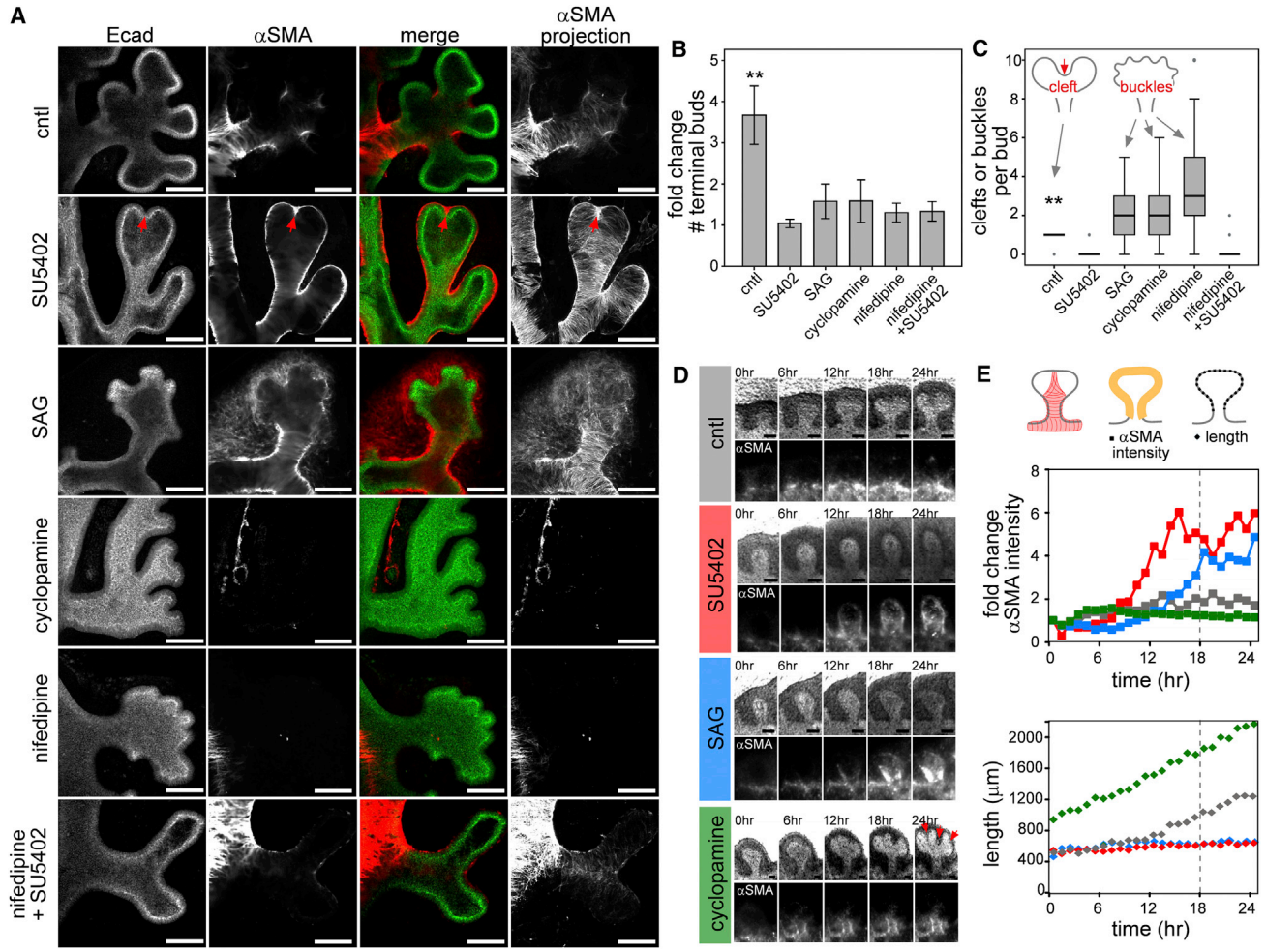


**Figure 3. Pharmacologically Disrupting Patterned Smooth Muscle Differentiation Blocks Terminal Bifurcation**

(A) Lung explants treated with SU5402 (5 μM), SAG (1 μg/ml), cyclopamine (1 μM), or nifedipine (10 μM). SU5402 was added after 24 hr of treatment with nifedipine for the "nifedipine + SU5402" condition. Fixed lungs were stained for E-cadherin and αSMA. Scale bars, 100 μm. Cntl, control.

(B and C) Disrupting the pattern of smooth muscle differentiation (B) disrupts terminal bifurcation and (C) induces epithelial buckling. (B) Shown are mean ± SD for five independent experiments. (C) The box-and-whiskers plot shows median, interquartile range, maxima, and minima. **$p < 0.01$.

(D) Snapshots from time-lapse movies of αSMA-RFP lung explants treated with SU5402, SAG, or cyclopamine. Scale bars, 100 μm.

(E) Quantification of αSMA intensity and epithelial length around the perimeter of the bud from time-lapse movies in (D).

See also Figure S3 and Movie S4.

terminal bifurcation of the epithelium (Figure 3B), and surprisingly led to the formation of shallow buckles along the surface of the buds (Figure 3C). The morphology of the buckled epithelium was distinct for each treatment despite the similar inhibition of smooth muscle differentiation (Figure S3D). Furthermore, the buckles that formed as a result of treatment with nifedipine were blocked by simultaneously inducing ectopic smooth muscle differentiation along the airway epithelium with SU5402 (Figures 3A–3C), suggesting that the presence of smooth muscle, not its contractility, shapes the epithelial bud during terminal bifurcation. Quantitative morphometric analysis of time-lapse movies of explants from αSMA-RFP embryos (Figure 3D; Movie S4) revealed that, as might be expected, drug treatments affected both the rate of smooth muscle differentiation and the rate of epithelial growth (Figure 3E). Inhibiting FGFR or activating SHH accelerated smooth muscle differentiation while simultaneously halting epithelial growth. Conversely, disrupting SHH halted smooth muscle differentiation while accelerating epithelial growth.

To directly modulate smooth muscle differentiation without altering signaling in the airway epithelium, we used an adenoviral approach to augment or reduce the levels of serum response factor (SRF) in the mesenchyme. Recombinant adenovirus only transduced the mesenchyme (Figure S4A), consistent with work by others showing that embryonic epithelium is refractory to adenovirus (Hsu et al., 2012). Ectopic expression of SRF throughout the mesenchyme (Figures S4B and S4C) led to disorganized differentiation of smooth muscle cells (Figure 4A) and elevated levels of smooth muscle markers (Figure 4B). Conversely, short hairpin RNA (shRNA)-mediated depletion of SRF (Figure S4B) blocked smooth muscle differentiation around the growing epithelium (Figures 4A and 4B; Figure S4D).

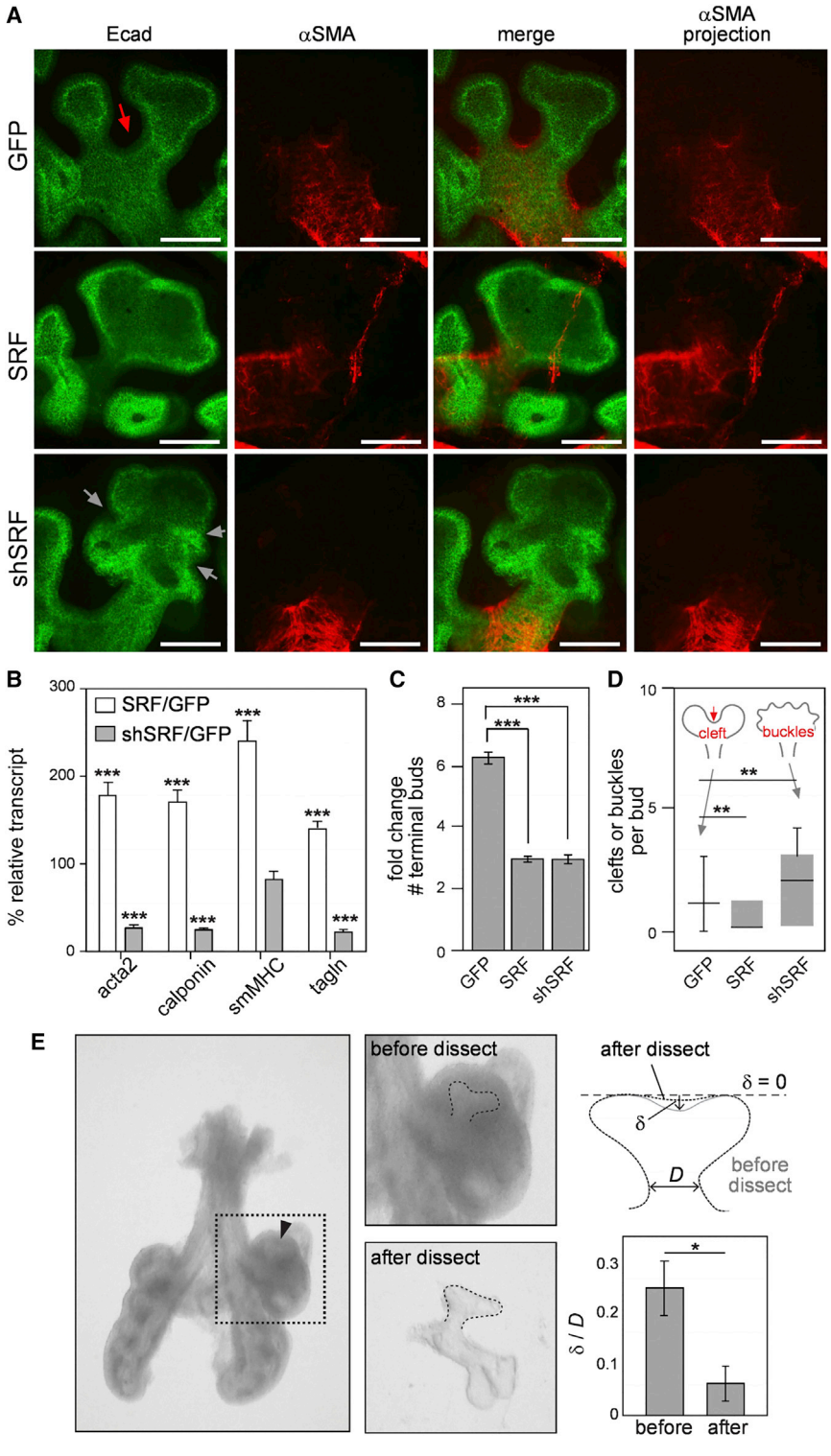


**Figure 4. Specifically Targeting the Airway Smooth Muscle Blocks Terminal Bifurcation**

(A) Lung explants transduced with AdGFP, AdSRF, or AdshSRF. Fixed lungs were stained for E-cadherin (Ecad) and αSMA. The red arrow indicates bifurcation; gray arrowheads indicate buckling. Scale bars, 100 μm.

(B) Relative transcript levels for markers of smooth muscle differentiation in explants transduced with AdSRF or AdshSRF. Shown are mean ± SD for three independent experiments. ***$p < 0.001$.

(C and D) Disrupting SRF levels (C) disrupts terminal bifurcation and (D) induces epithelial buckling. (C) Shown are mean ± SEM for three independent experiments. (D) The box-and-whiskers plot shows median, interquartile range, maxima, and minima. **$p < 0.01$; ***$p < 0.001$.

(E) Bright-field images of lung explant before and after dissecting off the mesenchyme from a stage 3 bud. The graph indicates the depth of the cleft before and after surgical removal of the smooth muscle. Shown are mean ± SEM for five independent experiments. *$p < 0.05$.

See also Figure S4.

Both manipulations completely prevented terminal bifurcation (Figure 4C), with SRF depletion inducing epithelial buckling (Figure 4D). Consistently, surgically removing the mesenchyme from the epithelium at a stage immediately after cleft formation (stage 3) caused the epithelium to pop back into a flattened (stage 2) morphology (Figure 4E), suggesting that the initial cleft is sculpted physically by the mesenchyme. Localized differentiation of airway smooth muscle thus appears to be required for terminal bifurcation during branching morphogenesis of the epithelium in the embryonic mouse lung.

## DISCUSSION

As the lung branches, a subpopulation of mesenchymal cells differentiate into smooth muscle that tightly surrounds the airway epithelium in a proximal to distal direction (Kumar et al., 2014). Although its existence in the embryonic mammalian lung has been recognized for over a decade (Tollet et al., 2001), the role of airway smooth muscle in epithelial branching has largely been ignored (Mitzner, 2004). Similar patterns of smooth muscle development have been noted in other branching organs. In the neonatal prostate of the rat, the smooth muscle layer around the ducts is noticeably thicker proximally and thins distally (Hayward et al., 1996). In the pubertal murine mammary gland, the myoepithelium surrounds the extending ducts, as well as the neck of the terminal end buds (Warburton et al., 1982), and time-lapse analysis of mammary organoids revealed that myoepithelial cells frequently localize to sites of bifurcation (Ewald et al., 2008). Whether these localized patterns of smooth muscle or myoepithelial cells direct epithelial bifurcation in the prostate or mammary gland remains to be determined, but our data show a clear role for localized smooth

muscle differentiation in terminal bifurcation of the airway epithelium. Our time-lapse analysis revealed remarkable dynamics of αSMA-positive cells, which appear at the midline of epithelial buds prior to the formation of any noticeable clefts. Importantly, any perturbation in the stereotyped pattern of smooth muscle differentiation prevented terminal bifurcation of the epithelium. Because transgenic knockout of smooth muscle is embryonic lethal (Hines et al., 2013), organ-specific genetic modulations will be required for definitive understanding of the role for visceral smooth muscle in epithelial morphogenesis.

Nonetheless, the spatiotemporal dynamics of airway smooth muscle cells suggest that they behave as a girdle around the bifurcating epithelial bud. As the airway epithelium grows, this girdle-like smooth muscle may constrain the epithelial tube at specific locations to direct the epithelial bifurcation. This conclusion is supported by our dissection experiments, which show that removing smooth muscle relaxes the epithelial cleft. The locations of smooth muscle around the bud neck and bifurcating cleft coincide with dense regions of extracellular matrix in the basement membrane of the lung (Liu et al., 2004; Mollard and Dziadek, 1998; Moore et al., 2005). Moreover, the overlapping patterns of smooth muscle and matrix are similar to the patterns of fibronectin observed at cleft sites in the branching salivary gland, suggesting a potential role for smooth muscle in regulating epithelial cell-cell adhesions during terminal bifurcation (Larsen et al., 2006; Sakai et al., 2003). In addition to these physical roles, the tightly packed smooth muscle could serve as a barrier to the diffusion of molecules between the epithelium and the mesenchyme, thus tuning bidirectional signaling, as in the induction of prostate morphogenesis (Thomson et al., 2002). Regardless, in the absence of the smooth muscle landmark at the future cleft site, stereotyped branching is blocked and instead the growing epithelium buckles into the mesenchyme. This epithelial buckling could result from constrained epithelial growth (Varner et al., 2015) or from a reduction in intraluminal pressure, which is normally maintained by the aligned smooth muscle around the circumference of the epithelial tube (Featherstone et al., 2005; Jesudason et al., 2005).

How airway smooth muscle differentiation is directed to the midline of the expanding epithelial bud is unclear. Several signaling molecules have been found to regulate the differentiation of smooth muscle adjacent to the proximal airway epithelium. FGF10-positive cells in the distal mesenchyme give rise to the smooth muscle cell population (Mailleux et al., 2005), whereas FGF9 secreted by the mesothelium simultaneously inhibits differentiation of smooth muscle to restrict its localization to the proximal airway (Yi et al., 2009). In addition, SHH signaling from the airway epithelium induces smooth muscle differentiation within the neighboring mesenchyme (Weaver et al., 2003; White et al., 2006). Whether and how these signals act as guidance cues for precisely patterned smooth muscle differentiation remains unclear. Further investigations are required to unlock the relationship between this physical mediator of airway branching and known genetic controls.

Airway epithelial branching morphogenesis is stereotyped in the mouse (Metzger et al., 2008). Thousands of budding events are thought to follow three simple genetically encoded subroutines to build recursively the complex branching structure of the lung, yet how the budding process is restricted to specific times and locations remains a mystery. The close spatiotemporal coincidence of smooth muscle differentiation and epithelial bifurcation suggests a physical or signaling role for stereotyped differentiation of the mesenchyme in the shaping of the airway epithelium. It will be interesting to determine whether stereotyped smooth muscle differentiation is controlled by the same genetically encoded subroutines as epithelial branching morphogenesis. Given the prevalence of smooth muscle around branching epithelial tissues, spatiotemporally patterned smooth muscle differentiation may represent a general physical strategy to sculpt complex epithelial architectures.

## EXPERIMENTAL PROCEDURES

### Mice

Timed-pregnant CD1 mice were obtained from Charles River. Breeding of αSMA-RFP transgenic reporter mice (Magness et al., 2004) and isolation of embryos were carried out in accordance with institutional guidelines following the NIH Guide for the Care and Use of Laboratory Animals and approved by the Mayo Clinic's Institutional Animal Care and Use Committee.

### Organ Culture

Ex vivo culture of embryonic lungs was performed following previously described protocols (Carraro et al., 2010). Briefly, lungs from *E*12 mouse embryos were dissected in PBS supplemented with antibiotics (50 units/ml of penicillin and streptomycin; Invitrogen) and cultured on porous membranes (nucleopore polycarbonate track-etch membrane, 8 μm pore size, 25 mm diameter; Whatman) in DMEM/F12 medium (without HEPES) supplemented with 5% fetal bovine serum (FBS, heat inactivated; Atlanta Biologicals) and antibiotics (50 units/ml of penicillin and streptomycin). Reagents used to perturb the pattern of smooth muscle and vascular endothelial differentiation included cyclopamine (1 or 2 μM; Tocris), nifedipine (10 μM; Sigma), SU5402 (5 or 10 μM; Santa Cruz), SU5416 (50 μM; Cayman Chemical), and SAG (1 or 2 μg/ml; Calbiochem). To disrupt smooth muscle differentiation specifically, lung explants were transduced with custom recombinant adenoviruses (Vector Biolabs)—adenovirus encoding GFP and SRF (AdSRF), GFP and shRNA against SRF (AdshSRF), or GFP alone (AdGFP)—for 48 hr. To surgically remove the mesenchyme, explants were incubated in 10 units/ml of dispase (Invitrogen) on ice for 15 min. The reaction was quenched by submerging the explants in FBS for 10 min. The explants were then transferred to a dissection dish containing PBS, and the mesenchyme was removed manually using fine tungsten needles (Del Moral and Warburton, 2010).

### Immunofluorescence Staining and Imaging

Lung explants were fixed with 4% paraformaldehyde in PBS for 15 min at room temperature followed by washing with 0.3% Triton X-100 in PBS and blocking with 10% goat serum. Samples were incubated with primary antibodies against E-cadherin (Invitrogen), αSMA (Sigma), or PECAM (rat anti-mouse CD31; BD Biosciences), followed by Alexa Fluor-conjugated secondary antibodies and nuclear counter-staining with Hoechst 33342 (Invitrogen). Stained lungs were dehydrated and cleared with Murray's clear (1:2 ratio of benzyl alcohol to benzyl benzoate; Sigma) and confocal images were collected using a spinning disk confocal (Bio-Rad) fitted to an inverted microscope. For live imaging, explants were cultured over porous membranes within custom-made glass bottom culture dishes within a stage-top incubator (Pathology Devices). The morphology of the explants was monitored every 24 hr under bright field on an inverted microscope (Nikon Ti).

### Image Analysis and Statistics

Quantitative image analysis and image projections were completed using ImageJ (Schneider et al., 2012). The orientation of smooth muscle cells in the neck and bud regions of at least three different lungs for each treatment were calculated using the OrientationJ plugin (Rezakhaniha et al., 2012). To quantify differences in branching, the fold-change in the number of terminal buds was determined by counting the terminal buds at the end of the experiment and normalizing to the number at time zero for each explant. To

characterize effects on terminal bifurcation per se, the total number of clefts (or buckles) for each bud was counted at the end of the culture period. ANOVA was conducted using IBM SPSS Statistics 19 for comparisons among different treatments.

### qRT-PCR Analysis

Total RNA from cultured lung explants was isolated using the QIAGEN RNeasy fibrous tissue mini kit and reverse-transcribed using the Verso cDNA synthesis kit (Thermo Scientific) according to manufacturer's instructions. qRT-PCR was performed using the Bio-Rad Mini Opticon instrument and iTaq Universal SYBR Green Supermix (Bio-Rad). Amplification was followed by melting curve analysis to verify the presence of a single PCR product. The expression level of each mRNA was normalized to that of 18S in the same sample. Primer sequences are listed in Supplemental Experimental Procedures.

## SUPPLEMENTAL INFORMATION

Supplemental Information includes Supplemental Experimental Procedures, four figures, and four movies and can be found with this article online at http://dx.doi.org/10.1016/j.devcel.2015.08.012.

## AUTHOR CONTRIBUTIONS

Conceptualization, H.Y.K. and C.M.N.; Methodology, H.Y.K., M.-F.P., and V.D.V.; Investigation, H.Y.K., M.-F.P., V.D.V., L.K., and E.M.; Writing, H.Y.K., D.C.R., and C.M.N.; Resources, D.C.R.; Project Administration, C.M.N.

## ACKNOWLEDGMENTS

This work was supported in part by grants from the NIH (GM083997, HL110335, HL118532, and HL120142), the NSF (CMMI-1435853), the David and Lucile Packard Foundation, the Alfred P. Sloan Foundation, the Camille and Henry Dreyfus Foundation, and Susan G. Komen for the Cure. C.M.N. holds a Career Award at the Scientific Interface from the Burroughs Wellcome Fund. M.-F.P. was supported in part by a postdoctoral fellowship from the Swedish Society for Medical Research (SSMF). L.K. was supported in part by the Lidow Senior Thesis Fund.

Received: March 20, 2013
Revised: July 10, 2015
Accepted: August 14, 2015
Published: September 17, 2015

## REFERENCES

Alescio, T., and Cassini, A. (1962). Induction in vitro of tracheal buds by pulmonary mesenchyme grafted on tracheal epithelium. J. Exp. Zool. *150*, 83–94.

Carraro, G., del Moral, P.-M., and Warburton, D. (2010). Mouse embryonic lung culture, a system to evaluate the molecular mechanisms of branching. J. Vis. Exp. *40*, 2035.

Chen, J.K., Taipale, J., Cooper, M.K., and Beachy, P.A. (2002a). Inhibition of Hedgehog signaling by direct binding of cyclopamine to Smoothened. Genes Dev. *16*, 2743–2748.

Chen, J.K., Taipale, J., Young, K.E., Maiti, T., and Beachy, P.A. (2002b). Small molecule modulation of Smoothened activity. Proc. Natl. Acad. Sci. USA *99*, 14071–14076.

Del Moral, P.M., and Warburton, D. (2010). Explant culture of mouse embryonic whole lung, isolated epithelium, or mesenchyme under chemically defined conditions as a system to evaluate the molecular mechanism of branching morphogenesis and cellular differentiation. Methods Mol. Biol. *633*, 71–79.

Ewald, A.J., Brenot, A., Duong, M., Chan, B.S., and Werb, Z. (2008). Collective epithelial migration and cell rearrangements drive mammary branching morphogenesis. Dev. Cell *14*, 570–581.

Featherstone, N.C., Jesudason, E.C., Connell, M.G., Fernig, D.G., Wray, S., Losty, P.D., and Burdyga, T.V. (2005). Spontaneous propagating calcium waves underpin airway peristalsis in embryonic rat lung. Am. J. Respir. Cell Mol. Biol. *33*, 153–160.

Fong, T.A.T., Shawver, L.K., Sun, L., Tang, C., App, H., Powell, T.J., Kim, Y.H., Schreck, R., Wang, X., Risau, W., et al. (1999). SU5416 is a potent and selective inhibitor of the vascular endothelial growth factor receptor (Flk-1/KDR) that inhibits tyrosine kinase catalysis, tumor vascularization, and growth of multiple tumor types. Cancer Res. *59*, 99–106.

Grobstein, C. (1953). Inductive epitheliomesenchymal interaction in cultured organ rudiments of the mouse. Science *118*, 52–55.

Havrilak, J.A., and Shannon, J.M. (2015). Branching of lung epithelium in vitro occurs in the absence of endothelial cells. Dev. Dyn. *244*, 553–563.

Hayward, S.W., Baskin, L.S., Haughney, P.C., Foster, B.A., Cunha, A.R., Dahiya, R., Prins, G.S., and Cunha, G.R. (1996). Stromal development in the ventral prostate, anterior prostate and seminal vesicle of the rat. Acta Anat. (Basel) *155*, 94–103.

Hines, E.A., Jones, M.K., Verheyden, J.M., Harvey, J.F., and Sun, X. (2013). Establishment of smooth muscle and cartilage juxtaposition in the developing mouse upper airways. Proc. Natl. Acad. Sci. USA *110*, 19444–19449.

Hsu, J.C., Di Pasquale, G., Harunaga, J.S., Onodera, T., Hoffman, M.P., Chiorini, J.A., and Yamada, K.M. (2012). Viral gene transfer to developing mouse salivary glands. J. Dent. Res. *91*, 197–202.

Jesudason, E.C., Smith, N.P., Connell, M.G., Spiller, D.G., White, M.R.H., Fernig, D.G., and Losty, P.D. (2005). Developing rat lung has a sided pacemaker region for morphogenesis-related airway peristalsis. Am. J. Respir. Cell Mol. Biol. *32*, 118–127.

Kumar, M.E., Bogard, P.E., Espinoza, F.H., Menke, D.B., Kingsley, D.M., and Krasnow, M.A. (2014). Mesenchymal cells: defining a mesenchymal progenitor niche at single-cell resolution. Science *346*, 1258810.

Larsen, M., Wei, C., and Yamada, K.M. (2006). Cell and fibronectin dynamics during branching morphogenesis. J. Cell Sci. *119*, 3376–3384.

Lazarus, A., Del-Moral, P.M., Ilovich, O., Mishani, E., Warburton, D., and Keshet, E. (2011). A perfusion-independent role of blood vessels in determining branching stereotypy of lung airways. Development *138*, 2359–2368.

Lewis, M.R. (1924). Spontaneous rhythmical contraction of the muscles of the bronchial tubes and air sacs of the chick embryo. Am. J. Physiol. *68*, 385–388.

Liu, Y., Stein, E., Oliver, T., Li, Y., Brunken, W.J., Koch, M., Tessier-Lavigne, M., and Hogan, B.L.M. (2004). Novel role for Netrins in regulating epithelial behavior during lung branching morphogenesis. Curr. Biol. *14*, 897–905.

Magness, S.T., Bataller, R., Yang, L., and Brenner, D.A. (2004). A dual reporter gene transgenic mouse demonstrates heterogeneity in hepatic fibrogenic cell populations. Hepatology *40*, 1151–1159.

Mailleux, A.A., Kelly, R., Veltmaat, J.M., De Langhe, S.P., Zaffran, S., Thiery, J.P., and Bellusci, S. (2005). Fgf10 expression identifies parabronchial smooth muscle cell progenitors and is required for their entry into the smooth muscle cell lineage. Development *132*, 2157–2166.

McCray, P.B., Jr. (1993). Spontaneous contractility of human fetal airway smooth muscle. Am. J. Respir. Cell Mol. Biol. *8*, 573–580.

McCulley, D., Wienhold, M., and Sun, X. (2015). The pulmonary mesenchyme directs lung development. Curr. Opin. Genet. Dev. *32*, 98–105.

Metzger, R.J., and Krasnow, M.A. (1999). Genetic control of branching morphogenesis. Science *284*, 1635–1639.

Metzger, R.J., Klein, O.D., Martin, G.R., and Krasnow, M.A. (2008). The branching programme of mouse lung development. Nature *453*, 745–750.

Mitzner, W. (2004). Airway smooth muscle: the appendix of the lung. Am. J. Respir. Crit. Care Med. *169*, 787–790.

Mohammadi, M., McMahon, G., Sun, L., Tang, C., Hirth, P., Yeh, B.K., Hubbard, S.R., and Schlessinger, J. (1997). Structures of the tyrosine kinase domain of fibroblast growth factor receptor in complex with inhibitors. Science *276*, 955–960.

Mollard, R., and Dziadek, M. (1998). A correlation between epithelial proliferation rates, basement membrane component localization patterns, and morphogenetic potential in the embryonic mouse lung. Am. J. Respir. Cell Mol. Biol. *19*, 71–82.

Moore, K.A., Polte, T., Huang, S., Shi, B., Alsberg, E., Sunday, M.E., and Ingber, D.E. (2005). Control of basement membrane remodeling and epithelial branching morphogenesis in embryonic lung by Rho and cytoskeletal tension. Dev. Dyn. *232*, 268–281.

Morrisey, E.E., and Hogan, B.L.M. (2010). Preparing for the first breath: genetic and cellular mechanisms in lung development. Dev. Cell *18*, 8–23.

Radzikinas, K., Aven, L., Jiang, Z., Tran, T., Paez-Cortez, J., Boppidi, K., Lu, J., Fine, A., and Ai, X. (2011). A Shh/miR-206/BDNF cascade coordinates innervation and formation of airway smooth muscle. J. Neurosci. *31*, 15407–15415.

Rezakhaniha, R., Agianniotis, A., Schrauwen, J.T., Griffa, A., Sage, D., Bouten, C.V., van de Vosse, F.N., Unser, M., and Stergiopulos, N. (2012). Experimental investigation of collagen waviness and orientation in the arterial adventitia using confocal laser scanning microscopy. Biomech. Model. Mechanobiol. *11*, 461–473.

Roman, J. (1995). Effects of calcium channel blockade on mammalian lung branching morphogenesis. Exp. Lung Res. *21*, 489–502.

Sakai, T., Larsen, M., and Yamada, K.M. (2003). Fibronectin requirement in branching morphogenesis. Nature *423*, 876–881.

Schachtner, S.K., Wang, Y., and Scott Baldwin, H. (2000). Qualitative and quantitative analysis of embryonic pulmonary vessel formation. Am. J. Respir. Cell Mol. Biol. *22*, 157–165.

Schittny, J.C., Miserocchi, G., and Sparrow, M.P. (2000). Spontaneous peristaltic airway contractions propel lung liquid through the bronchial tree of intact and fetal lung explants. Am. J. Respir. Cell Mol. Biol. *23*, 11–18.

Schnatwinkel, C., and Niswander, L. (2013). Multiparametric image analysis of lung-branching morphogenesis. Dev. Dyn. *242*, 622–637.

Schneider, C.A., Rasband, W.S., and Eliceiri, K.W. (2012). NIH Image to ImageJ: 25 years of image analysis. Nat. Methods *9*, 671–675.

Sparrow, M.P., and Lamb, J.P. (2003). Ontogeny of airway smooth muscle: structure, innervation, myogenesis and function in the fetal lung. Respir. Physiol. Neurobiol. *137*, 361–372.

Thomson, A.A., Timms, B.G., Barton, L., Cunha, G.R., and Grace, O.C. (2002). The role of smooth muscle in regulating prostatic induction. Development *129*, 1905–1912.

Tollet, J., Everett, A.W., and Sparrow, M.P. (2001). Spatial and temporal distribution of nerves, ganglia, and smooth muscle during the early pseudoglandular stage of fetal mouse lung development. Dev. Dyn. *221*, 48–60.

Unbekandt, M., del Moral, P.-M., Sala, F.G., Bellusci, S., Warburton, D., and Fleury, V. (2008). Tracheal occlusion increases the rate of epithelial branching of embryonic mouse lung via the FGF10-FGFR2b-Sprouty2 pathway. Mech. Dev. *125*, 314–324.

Varner, V.D., Gleghorn, J.P., Miller, E., Radisky, D.C., and Nelson, C.M. (2015). Mechanically patterning the embryonic airway epithelium. Proc. Natl. Acad. Sci. USA *112*, 9230–9235.

Warburton, M.J., Mitchell, D., Ormerod, E.J., and Rudland, P. (1982). Distribution of myoepithelial cells and basement membrane proteins in the resting, pregnant, lactating, and involuting rat mammary gland. J. Histochem. Cytochem. *30*, 667–676.

Weaver, M., Batts, L., and Hogan, B.L.M. (2003). Tissue interactions pattern the mesenchyme of the embryonic mouse lung. Dev. Biol. *258*, 169–184.

White, A.C., Xu, J., Yin, Y., Smith, C., Schmid, G., and Ornitz, D.M. (2006). FGF9 and SHH signaling coordinate lung growth and development through regulation of distinct mesenchymal domains. Development *133*, 1507–1517.

Yi, L., Domyan, E.T., Lewandoski, M., and Sun, X. (2009). Fibroblast growth factor 9 signaling inhibits airway smooth muscle differentiation in mouse lung. Dev. Dyn. *238*, 123–137.